Time-Dependence of the Electron Energy Distribution Function in the Nitrogen Afterglow

Vasco Guerra, Francisco M. Dias, Jorge Loureiro, Paulo Araújo Sá, Philippe Supiot, Chrsitian Dupret, and Tsviatko Popov

***Abstract*—In this paper, we present an investigation of the time-relaxation of the electron energy distribution function (EEDF) in the nitrogen afterglow of an $\omega/2\pi = 433$ MHz flowing discharge at $p = 3.3$ torr, in a tube with inner radius $R = 1.9$ cm. We solve the time-dependent Boltzmann equation, including the term for creation of new electrons in associative/Penning reactions, coupled to a system of rate balance equations for the heavy-particles. The EEDFs are also obtained experimentally, from second derivatives of digitized probe characteristics measured using a triple probe technique, and compared with the calculations. It is shown that an equilibrium between the vibrational distribution function of ground-state molecules $N_2(X\,^1\Sigma_g^+, v)$ and low-energy electrons is rapidly established, in times $\sim 10^{-7}$ s. In these early instants of the postdischarge, a dip is formed in the EEDF around 4 eV. The EEDF finally reaches a quasi-stationary state for $t \gtrsim 10^{-6}$ s, although the electron density still continues to decrease beyond this instant. Collisions of highly excited $N_2(X\,^1\Sigma_g^+, v \gtrsim 35)$ molecules with $N(^4S)$ atoms are in the origin of a maximum in the electron density occurring downstream from the discharge at $\simeq 2 \times 10^{-2}$ s. These reactions create locally the metastable states $N_2(A\,^3\Sigma_u^+)$ and $N_2(a'\,^1\Sigma_u^-)$, which in turn ionize the gas in associative/Penning processes. Slow electrons remain for very long times in the postdischarge and can be involved in electron stepwise processes with energy thresholds smaller than $\sim$2–3 eV.**

***Index Terms*—Nitrogen, afterglow, electron energy distribution function (EEDF), relaxation, kinetic model.**

I. Introduction

NITROGEN flowing postdischarges have been found to be useful in different applications, such as N atoms production for metallic nitriding [1] and for polymer surface treatments [2]. A complete understanding of how the main plasma parameters change in the afterglow is, therefore, of primary importance for plasma processing design and optimization. A crucial aspect is the knowledge of the time-dependent variation of the electron energy distribution function (EEDF), since the EEDF allows to evaluate the decay of the electron mean energy and density, as well as to precisely characterize the main mechanisms involved in electron energy losses. One strongly marked situation is the presence of electrons at times as large as few ms as it occurs in the so-called short-lived afterglow (SLA) [3], [4].

To our knowledge, there are not many studies devoted to the experimental determination of the EEDF in N_2 afterglow plasmas, especially when they exhibit a SLA. The first attempts to characterize the electrons in a nitrogen postdischarge dealt with 2450-MHz microwave discharges induced in small-diameter discharge tubes (12 mm) and were performed by double floating probes [5] or using a resonant microwave cavity [6]. These first works have provided at most electron densities. The measured values, $10^8 - 7 \times 10^9$ cm^{-3}, were consistent with each other for comparable systems, but assuming maxwellian EEDFs by default. Broida [5] obtained the values of the electron temperature as well, in the range 0.6–0.9 eV. Later on, Chen and Gooddings [7] made experiments giving access to the electron energy, by use of a triple probe technique, but no counter experiment was done to confirm their results, not even under similar conditions. EEDF measurements have been finally reported in low-pressure pulsed discharges in [8]–[10]. A couple of years later, a dip structure of the EEDF was observed in the 4-eV electron energy region in [11], whereas recent measurements have been published in [12]. A few studies have been conducted as well on the variation of the electron density n_e in decaying nitrogen plasmas [13]–[16], and the existence of a no-monotonic variation of n_e in nitrogen postdischarges was pointed out in [13] and [16]. These works have shown that the electron density has an initial stage of decrease, but then an increase occurs during a relatively long period, after which the plasma finally dies out. This very same behavior is presented also by some heavy-particles in the postdischarge, such as $N_2(A\,^3\Pi_g)$ and $N_2(B\,^3\Pi_g)$ molecules [16] and $N_2^+(B\,^2\Sigma_u^+)$ ions [17].

The theoretical analysis of the EEDF in the afterglow have started with the works of Capitelli and co-workers [18], [8], devoted to the coupling between the EEDF and the vibrational distribution function (VDF) of $N_2(X\,^1\Sigma_g^+, v)$ molecules, and in a second stage also with the kinetics of electronically excited states. Later on, a Monte Carlo model was developed in [20], in which the loss of electrons was taken into account assuming a constant ambipolar diffusion coefficient. Recently, we have developed a model to study the transition from ambipolar to free diffusion regimes occurring in the afterglow [21], [22] by solving the time-dependent electron Boltzmann equation including a term describing the continuous reduction of the space-charge field [23]. The theoretical analysis developed in [23] includes a first module with a self-consistent description of the

Manuscript received October 31, 2002; revised January 10, 2003. This work was carried out under a scientific cooperation agreement between the Instituto de Cooperação Científica e Tecnológica Internacional—Portugal and the Ambassade de France—France under Project n° 440 B1.

V. Guerra, F. M. Dias, and J. Loureiro are with the Centro de Física dos Plasmas, Instituto Superior Técnico, 1049-001 Lisboa, Portugal (e-mail: vguerra@theta.ist.utl.pt).

P. A. Sá is with the Dep. de Física, Faculdade de Engenharia, Universidade do Porto, 4200-465 Porto, Portugal.

P. Supiot and C. Dupret are with the Laboratoire de Génie des Procédés d'Interactions Fluides Réactifs-Matériaux, Univ. des Sciences et Technologies de Lille, 59655 Villeneuve d'Ascq Cédex, France.

T. Popov is with the Faculty of Physics, Sofia University, Sofia 1164, Bulgaria.

Digital Object Identifier 10.1109/TPS.2003.815485

discharge. The EEDF, thus obtained, is then used as the initial distribution for the afterglow.

In this paper, in parallel with measurements of the EEDF in the nitrogen afterglow, we improve the theoretical description considered in [23] by including the terms for creation of new electrons by Penning ionization, which explain the no-monotonic behavior of n_e reported in [13] and [16]. For this purpose, we couple the equations ruling the time-evolution of the heavy-particles with the time-dependent electron Boltzmann equation. The first results for the evolution of the populations of the heavy-particles in the postdischarge have already been reported in [24] and [25]. Once the temporal evolution of the heavy-particles is known, it can be introduced into the time-dependent electron Boltzmann equation, allowing the description of the production of new electrons. The theoretical model just described, although developed for a quite general case, provides a good interpretation of the complex phenomena occuring in the SLA experimentally characterized in [16] and [17]. This work is further complemented with the experimental determination of the EEDF at different instants in the afterglow, following the same procedure as in [12].

The conditions of the present study correspond to a nitrogen afterglow created by a microwave discharge operating at frequency $\omega/2\pi = 433$ MHz, pressure $p = 3.3$ torr, in a Pyrex tube of inner radius $R = 1.9$ cm. For these conditions, the electron density at the beginning of the postdischarge is estimated to be $n_e(0) = 3 \times 10^{10}$ cm^{-3} [16], which corresponds approximately to the critical value for a surface-wave propagation.

The organization of this paper is as follows. Section II describes the theoretical model used to study the electron kinetics in the nitrogen afterglow. The experimental method is briefly described in Section III. Section IV contains the results of this investigation with the corresponding discussion, in which the theoretical calculations are compared with the experimental results. Finally, Section V summarizes the main conclusions of this study.

II. Theoretical Model

The theoretical model used to investigate the evolution of the EEDF in the nitrogen afterglow is based on the one presented in [23], but with some important differences to be discussed. The study must begin with a self-consistent description of the discharge, since it is in the discharge that the starting conditions for the postdischarge are established. Accordingly, we developed a discharge model accounting for the electron and heavy-particle kinetics in DC or high-frequency (HF) fields, described in detail in [26]–[28]. Shortly, the homogeneous electron Boltzmann equation is coupled to a system of rate balance equations describing the populations of the vibrationally excited ground-state molecules $N_2(X\,^1\Sigma_g^+, v)$, the electronically excited states $N_2(A\,^3\Sigma_u^+, B\,^3\Pi_g, C\,^3\Pi_u, a'\,^1\Sigma_u^-, a\,^1\Pi_g, w\,^1\Delta_u, a''\,^1\Sigma_g^+)$, ground-state and metastable atoms $N(^4S, ^2D, ^2P)$ and N_2^+ and N_4^+ ions. The electric field sustaining the discharge is determined from the requirement that under steady-state conditions the total rate for ionization must compensate exactly the rate of loss of electrons by diffusion to the wall, under space-charge field effects, and electron-ion recombination. The rate for ionization includes electron impact ionization both from ground-state and electronically excited N_2 molecules, as well as through the associative/Penning reactions [26]

$$\begin{aligned} N_2(A\,^3\Sigma_u^+) + N_2(a'\,^1\Sigma_u^-) &\longrightarrow N_2(X\,^1\Sigma_g^+) + N_2^+ + e \\ &\longrightarrow N_4^+ + e \end{aligned} \tag{1}$$

and

$$\begin{aligned} N_2(a'\,^1\Sigma_u^-) + N_2(a'\,^1\Sigma_u^-) &\longrightarrow N_2(X\,^1\Sigma_g^+) + N_2^+ + e \\ &\longrightarrow N_4^+ + e. \end{aligned} \tag{2}$$

As shown in [26] and [27], these two reactions are the dominant mechanisms for ionization in a nitrogen discharge.

The set of electron cross sections used in the solution of the electron Boltzmann equation is essentially the one developed by Pitchford and Phelps [29], with a few additions described in detail in [30]. The excitation of electronic states was treated as a single energy loss process assuming, in this case, that all the molecules are in the ground vibrational level. The effect of considering individual $N_2(X, v{-}Y, v')$ transitions has been studied in [31]. On the other hand, the cross section for the excitation from $(X, v > 0)$ to $(X, w > v)$ was assumed identical in shape and magnitude to the one for the $0 \rightarrow w - v$ transition, but with a different threshold accounting for the anharmonicity of the oscillator. A comparison of this procedure with other hypotheses has been performed in [15], suggesting the correctness of the present approach. Nevertheless, there is still no absolute consensus in the literature for the choice of cross sections for electron collisions involving transitions between vibrational levels.

The input parameters for the discharge model are the field frequency $\omega/2\pi$, tube radius R, gas pressure p and the electron density at the end of the discharge $n_e(0)$. Notice that a traveling wave sustained discharge exhibits an axial structure, which can be described by coupling to the system of equations the ones describing the wave electrodynamics [32], [33]. In this case, one should use the electron density at the position of the launcher or the power delivered to the launcher as input parameter, instead of $n_e(0)$. However, since the goal of this paper is to investigate the afterglow we do not need to characterize the axial structure. It is in fact enough to consider the end of the discharge, where the initial conditions for the afterglow are determined. The critical value for the electron density $n_e(0)$ can be estimated from the wave-dispersion characteristics. The gas temperature can be also calculated from the model, as it was done in [27] and [33], but it will be taken here as an input parameter as well.

Once the EEDF at the end of the discharge is obtained, its evolution in the afterglow is ruled by the time-dependent Boltzmann equation, which can be written in the form [23]

$$\begin{aligned} &\frac{\partial F}{\partial t} + \frac{2}{3m}\frac{u}{\nu_c^e \Lambda^2}\frac{D_{se}}{D_e}F + \frac{1}{\sqrt{u}}\frac{\partial G}{\partial u} \\ &\quad = \frac{1}{\sqrt{u}}\sum_{i,j}[\sqrt{u+u_{ij}}\nu_{ij}(u+u_{ij})F(u+u_{ij}) - \sqrt{u}\nu_{ij}F \\ &\qquad + \sqrt{u-u_{ij}}\nu_{ji}(u-u_{ij})F(u-u_{ij}) - \sqrt{u}\nu_{ji}F] \\ &\qquad - \nu_{\rm rec}F + \frac{1}{\sqrt{u}}\sum_{i=1}^{2}\langle\nu_{\rm ion}^i\rangle\, n_e\delta(u_i). \end{aligned} \tag{3}$$

Here, $F(u,t)$ is the EEDF in the post discharge, with the normalization

$$\int_0^\infty F(u,t)\sqrt{u}\,du = n_e(t) \tag{4}$$

u and m are the electron energy and mass, ν_c^e is an effective collision frequency for momentum transfer [34], $\Lambda = R/2.405$ is the characteristic diffusion length for a cylindrical tube with radius R, D_{se} and D_e are the effective and free diffusion coefficients for electrons [23], $G(u)$ is the total electron flux in energy space due to the continuous terms in the Boltzmann equation. The effective diffusion coefficient is calculated from

$$D_{se} = D_a \frac{1+\Lambda^2/\lambda_D^2}{(D_a/D_e)+\Lambda^2/\lambda_D^2} \tag{5}$$

with D_a and λ_D denoting the ambipolar diffusion coefficient and the Debye length. $G(u)$ includes the terms for elastic collisions, inelastic and superelastic collisions of electrons with rotational levels in the continuous approximation and electron-electron collisions [23]. The electric field is set to zero in the postdischarge, so that G does not include the usual term for the flux driven by the applied field. The terms in the brackets in the right-hand side of (3) account for the excitation of vibrational and electronic states of N_2 by inelastic collisions (first and second terms) and of the de-excitation of the vibrational states by electron superelastic collisions (third and fourth terms), where u_{ij}, ν_{ij}, and ν_{ji} denote the energy threshold and the inelastic and superelastic collision frequencies, respectively. The last two terms in (3) describe the electron-loss process of dissociative recombination with frequency $\nu_{\rm rec}$ and the creation of new electrons. In the term for production of new electrons, $\langle\nu_{\rm ion}^i\rangle$— with $\mathrm{i} = 1, 2$ —represents the ionization frequency through the Penning reactions (1) and (2), respectively, defined effectively per electron as

$$\langle\nu_{\rm ion}^1\rangle = \frac{[\mathrm{N_2}(A)][\mathrm{N_2}(a')]}{n_e}k_1 \tag{6}$$

and

$$\langle\nu_{\rm ion}^2\rangle = \frac{[\mathrm{N_2}(a')][\mathrm{N_2}(a')]}{n_e}k_2 \tag{7}$$

with $k_1 = 10^{-11}$ cm^3/s and $k_2 = 5\times10^{-11}$ cm^3/s [26]. The new electrons are created with energies $u_1 = 0$ and $u_2 = 1.3$ eV, and the δ functions verify the usual normalization condition $\int_0^\infty \delta(u)\,du = 1$.

The inclusion in the Boltzmann equation of the production of new electrons constitutes a major improvement in the description of the electron kinetics in the nitrogen afterglow as compared with that presented in [23]. Besides processes (1) and (2), the importance of other mechanisms leading to electron production has been checked in the postdischarge, namely

$$\mathrm{N_2}(X\,{}^1\Sigma_g^+, v\geq 30) + \mathrm{N_2}(a'\,{}^1\Sigma_u^-) \longrightarrow \mathrm{N_2}(X\,{}^1\Sigma_g^+) + \mathrm{N_2^+} + e \tag{8}$$

and

$$\mathrm{N_2}(X\,{}^1\Sigma_g^+, v\geq 36) + \mathrm{N_2}(B\,{}^3\Pi_g) \longrightarrow \mathrm{N_2}(X\,{}^1\Sigma_g^+) + \mathrm{N_2^+} + e, \tag{9}$$

but their effect have been seen to be always very small. Without the formation of new electrons it is certainly impossible to describe the increase in n_e after an initial stage of decay, as observed in [13] and [16]. Furthermore, the analysis of the ionization mechanisms in the postdischarge leads naturally to a deeper understanding of the processes involving heavy-particles, due to the strong coupling existing between the electron and heavy-particle kinetics.

Inspection of (6) and (7) reveals the need to know the time-dependent concentrations $[\mathrm{N_2}(A)](t)$ and $[\mathrm{N_2}(a')](t)$ in the afterglow. For this purpose, we developed another module describing the relaxation of the heavy-particles that were considered in the discharge, using the discharge calculated populations as initial conditions for the afterglow. The basis of this model was presented in [35], but the description has been significantly improved in [36] and very recently in [25] and [37]. It includes the rate balance equation for all the species previously considered under discharge conditions, i.e., vibrational levels of ground-state molecules, the most important electronically excited states of N_2, ground-state and metastable atoms and the ionic species N_2^+ and N_4^+.

The detailed analysis of the heavy-particle kinetics is outside the scope of this paper, so that the reader should refer to the cited references for details. Nevertheless, it is worth stressing that $\mathrm{N_2}(A\,{}^3\Sigma_u^+)$ and $\mathrm{N_2}(a'\,{}^1\Sigma_u^-)$ metastables are created in the afterglow in collisions of N_2 vibrationally excited molecules in very high levels with N atoms, through the reactions

$$\mathrm{N_2}(X\,{}^1\Sigma_g^+, v\geq 39) + \mathrm{N}({}^4S) \longrightarrow \mathrm{N_2}(A\,{}^3\Sigma_u^+) + \mathrm{N}({}^2D) \tag{10}$$

and

$$\mathrm{N_2}(X\,{}^1\Sigma_g^+, v\geq 38) + \mathrm{N}({}^4S) \longrightarrow \mathrm{N_2}(a'\,{}^1\Sigma_u^-) + \mathrm{N}({}^4S). \tag{11}$$

The highly excited vibrational levels of ground-state N_2 molecules, which do not present a significant concentration under discharge conditions, can be effectively populated in the afterglow, as a consequence of the so-called V-V pumping up mechanism [38], [39]. That being so, there is a local production of $\mathrm{N_2}(A\,{}^3\Sigma_u^+)$ and $\mathrm{N_2}(a'\,{}^1\Sigma_u^-)$ molecules in the afterglow, which will be subsequently involved in the production of new electrons via reactions (1) and (2) [36], [25].

The calculated populations $[\mathrm{N_2}(A)](t)$ and $[\mathrm{N_2}(a')](t)$ are then introduced in the time-dependent Boltzmann (3), which is finally solved to obtain the EEDF and all the related quantities. It should be noted that the calculated time-dependent concentrations of the different heavy-particles during the postdischarge has shown that it is possible to assume a constant population of levels $[\mathrm{N_2}(X, v\leq 10)]$ during the resolution of the Boltzmann equation, for afterglow times lower than $\sim 10^{-2}$ s [25].

III. Experiment

The EEDFs were deduced from second derivatives of digitized probe characteristics measured using a triple probe technique. The experimental arrangement is shown in Fig. 1. The experiments were carried out for a discharge operating at frequency $\omega/2\pi = 433$ MHz, pressure $p = 3.3$ torr, in a Pyrex

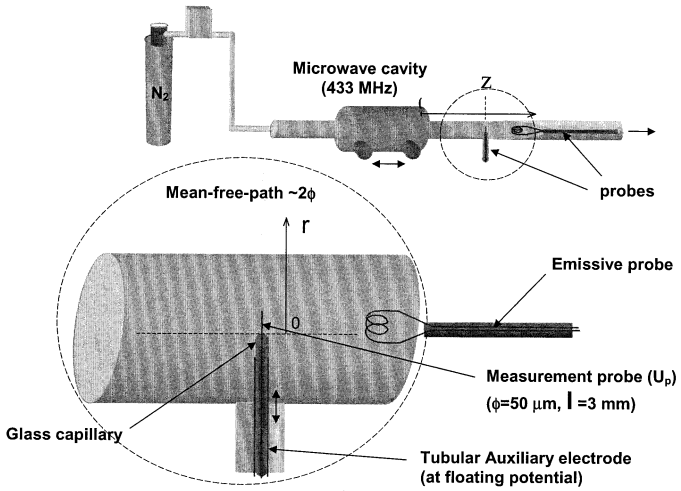

Fig. 1. Experimental setup for the measurement of the EEDF in the nitrogen afterglow.

tube of inner radius $R = 1.9$ cm. The discharge tube has been adapted in order to position the different components of the probe measurement set-up. A tungsten wire of 3-mm length and 50-μm radius forms the probe tip. The probe is supported by a glass capillary tube covered by a partially insulated stainless steel tube whose exposed region plays the role of auxiliary electrode. In order to minimize plasma and flow perturbations, the reference electrode was chosen to be an emissive one [40] and it was inserted downstream into the discharge tube while the probe enters radially through a Teflon sleeve which enables its radial movement under vacuum. Electrically, the active probe is connected to the input of a transimpedance amplifier (virtual ground) through a second order, anti-aliasing filter which also provides regularization without needing to record many probe characteristics in a systematic way. The sweeping potential is applied to the reference electrode. A PC-based data acquisition board digitizes the auxiliary electrode potential and the output from the above amplifier. Since an oscilloscope's analysis of the probe floating potential did not show any fluctuations at frequencies above the anti-aliasing filter cutoff, there was no need for probe compensation. Both the probe arrangement used and the numerical differentiation/averaging scheme (Hamming apparatus function with an adaptive size) are similar to those described in [41].

Since some current must flow into the finite input impedance of the data acquisition board, the auxiliary electrode potential deviates from the floating one in case of a nonnegligible sheath impedance. The value of this deviation is given by how much the auxiliary electrode should be biased below the floating potential in order to withdraw the above current from the plasma. This latter value can be readily obtained from an auxiliary electrode-plasma probe characteristic. In this line, the active probe and the auxiliary electrode role were interchanged and, at each position, two sets of voltage–current (*V-I*) characteristics were measured. The potential deviations were then derived from the *V-I* characteristics. The correction can be calculated using either simple algebra or numerically, depending on if it is small or large, respectively. All data presented in this paper satisfy the former condition.

As it is known, the second derivative of the probe characteristics is not EEDF representative when the electron free path and the probe radius are of the same order of magnitude. Mathematically speaking, to deduce the EEDF from probe measurements under collisional conditions requires that two coupled inverse problems are solved, since the distortion of the second derivative includes an integral over the unknown EEDF and the data is convoluted by the apparatus function. The situation is simpler when the EEDF can be assumed Maxwellian. Then, the problem solution requires only two unknown parameters, the electron density and temperature, which can be used as fitting parameters through a comparison between measured and theoretical probe characteristics [42]. However, under our experimental conditions, the probe current is clearly distorted by collisions (the mean free path is about twice the probe radius) and the assumption of a Maxwellian EEDF constitutes a rough approximation. So, we felt the need to devise a method to correct for the collisional effects on the second derivative of the probe characteristics. Basically, the theoretical probe characteristic corresponding to a seeded EEDF is obtained as in [43] and it is compared against the measured one. The corrections are iteratively introduced into the EEDF until an acceptable matching is achieved. The scaling factor between the theoretical and measured probe characteristics provides the value of the electron density. Details of this method can be found in [12].

IV. Results and Discussion

Except otherwise mentioned, the calculations were carried out for the plasma configuration described in the experimental section (discharge operating at frequency $\omega/2\pi = 433$ MHz, pressure $p = 3.3$ torr, in a Pyrex tube of inner radius $R = 1.9$ cm) with the electron density at the end of the discharge/beginning of the postdischarge estimated to be $n_e(0) = 3 \times 10^{10}$ cm^{-3} and the value of the gas temperature in the discharge to be approximately 1000 K. This set of parameters correspond to the experimental conditions of [16] and [17]. In this case, the calculated effective electric field [44] in the discharge is $E_e/N = 4.6 \times 10^{-16}$ V·cm^2 and the vibrational temperature of ground-state molecules T_V, defined here as the characteristic temperature of the Treanor-like distribution [38] that best fits the calculated VDF for the four lower vibrational levels, is close to 6200 K.

Fig. 2 shows the EEDF $f(u,t)$ during the afterglow, with t expressed in seconds. The EEDF is normalized to unity, $\int_0^\infty f(u)\sqrt{u}\,du = 1$, so that $F(u,t) = f(u,t)n_e(t)$. It is clearly seen that the EEDF is largely modified in the first instants of the afterglow ($t \lesssim 10^{-6}$ s), as a result of electron inelastic collisions. On the contrary, for times $t \gtrsim 10^{-6}$ s the EEDF attains a quasi-stationary state, which is due to an equilibrium achieved between the EEDF and the VDF, where the superelastic collisions of electrons with vibrationally excited molecules $N_2(X\,^1\Sigma_g^+, v)$ compensate for the inelastic vibrational losses [18], [23]. As mentioned before, in the present Boltzmann calculations the time variation of the concentrations of the states $N_2(A\,^3\Sigma_u^+)$ and $N_2(a'\,^1\Sigma_u^-)$ was taken into account, but the populations of the first ten levels of the VDF were assumed constant. This was recently shown to be

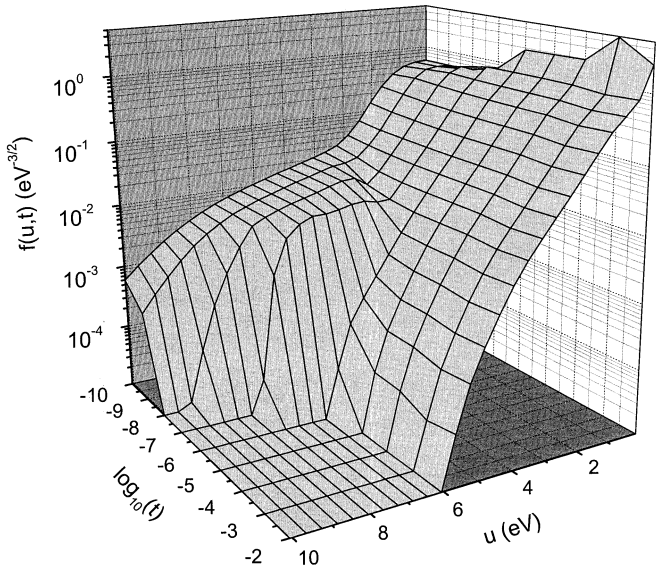

Fig. 2. Calculated EEDF in the nitrogen afterglow of a $\omega/2\pi = 433$ MHz discharge at $p = 3.3$ torr in a cylindrical tube with radius $R = 1.9$ cm. In the discharge, $E_e/N = 4.6 \times 10^{-16}$ V·cm^2 and $T_V = 6196$ K. The afterglow time t is expressed in seconds.

a good approximation for the conditions of this investigation up to times of the order of $10^{-3} - 10^{-2}$ s [25]. For longer times, the VDF starts to be modified in the low vibrational levels and any results shown here should be regarded merely as indicative.

A. Early Instants of the Afterglow: $t < 10^{-6}$ s

No measurements are available here for $t < 10^{-6}$ s, but it is worth to examine in some detail the relaxation of the EEDF in this region using the Boltzmann analysis. To examine its behavior in the early instants of the afterglow, $f(u,t)$ is plotted for $t = 10^{-9}, 10^{-8}$ and 10^{-7} s in Fig. 3. The first electronically excited states of N_2 is the triplet $N_2(A\,^3\Sigma_u^+)$, with an energy threshold of about 6.2 eV, and the rapid depletion of the high-energy tail of the distribution ($u \gtrsim 6$ eV) shown in Figs. 2 and 3 is, thus, a consequence of the inelastic collisions of the electrons with ground-state molecules.

One striking aspect revealed by Fig. 3 is the formation of a "dip" around $u \simeq 4$ eV for afterglow times in the range 10^{-8}–10^{-7} s (see also Fig. 2). This is a result of the particular shape of the electron cross sections for excitation of the vibrational levels $N_2(X\,^1\Sigma_g^+, v)$, which present a strong maximum at $u \simeq 2$ eV and vanish for $u \geq 4$ eV [30]. In order to clarify the processes leading to the formation of the dip, Fig. 4 shows the frequency $\nu(u)$ of gain or loss of electrons with a certain energy u, for $t = 10^{-9}$ s. A positive value of ν corresponds to gain of electrons, whereas a negative one means loss of electrons. The dotted curve represents the value of ν in inelastic and superelastic vibrational collisions, the dashed curve is for ν in inelastic collisions of excitation of the electronic states and the full curve is the total frequency ν of gain and loss of electrons (which is approximately the sum of the other two curves). It can be seen that the behavior of electrons with energies lower than 4 eV is determined almost exclusively by the inelastic and superelastic electron-vibration (e-V) collisions. As an outcome of this mechanism, there is a loss of electrons in the 2–4 eV energy range,

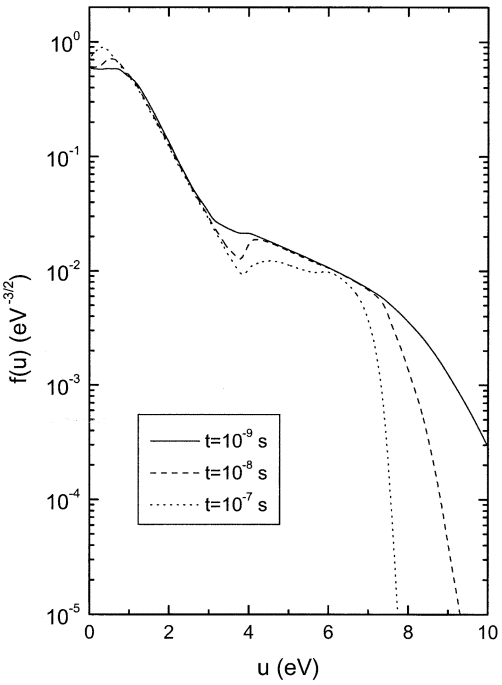

Fig. 3. Calculated EEDFs in the first instants of the afterglow, in the same conditions as in Fig. 1: at $t = 10^{-9}$ s (—); $t = 10^{-8}$ s (– –); and $t = 10^{-7}$ s ($\cdots$).

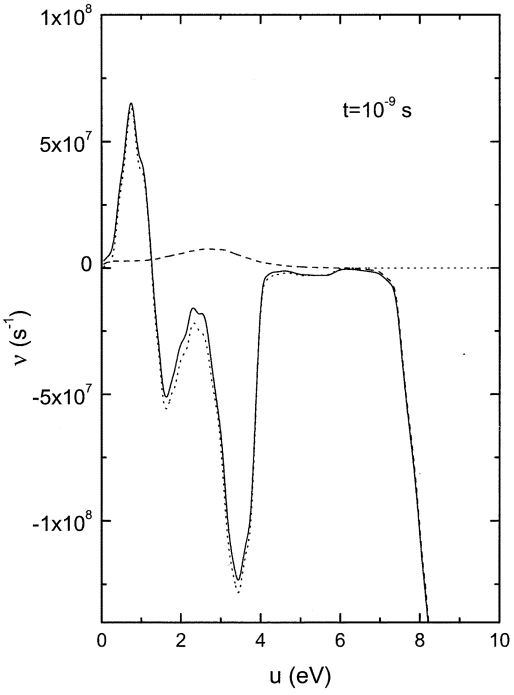

Fig. 4. Frequency of gain or loss of electrons as a function of their energy, in the same conditions as in Fig. 1, for $t = 10^{-9}$ s. Gain/loss due to the vibrational excitation and de-excitation ($\cdots$); due to the excitation of electronically excited states (– –); total frequency of gain/loss of electrons (—).

where the vibrational cross section is important, and a gain in the 0–2 eV one. On the other hand, electrons with energies between 4 and 6 eV do not lose appreciably their energy, since all the inelastic cross sections are zero in this range. In other words, the frequency for loss of electrons at $u \simeq 4$ eV is higher than the frequency for loss of electrons both at $u \simeq 2$–3 eV and $u \simeq 4$–6

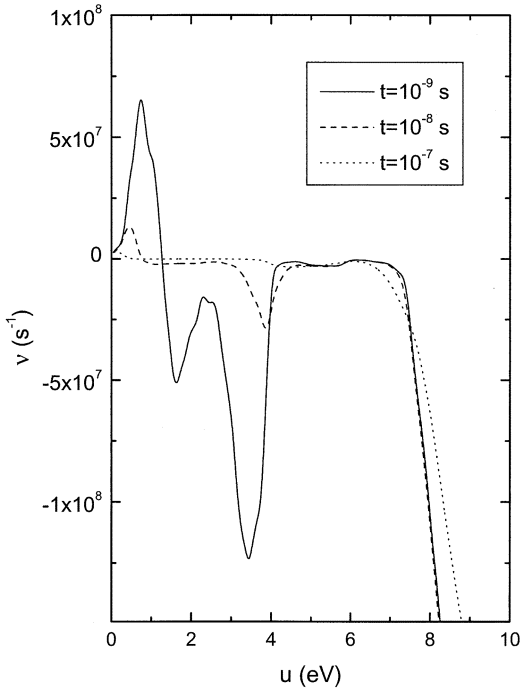

Fig. 5. Total frequency of gain or loss of electrons as a function of their energy, in the same conditions as in Fig. 1, for $t = 10^{-9}$ s (—); $t = 10^{-8}$ s (– –); and $t = 10^{-7}$ s ($\cdots$).

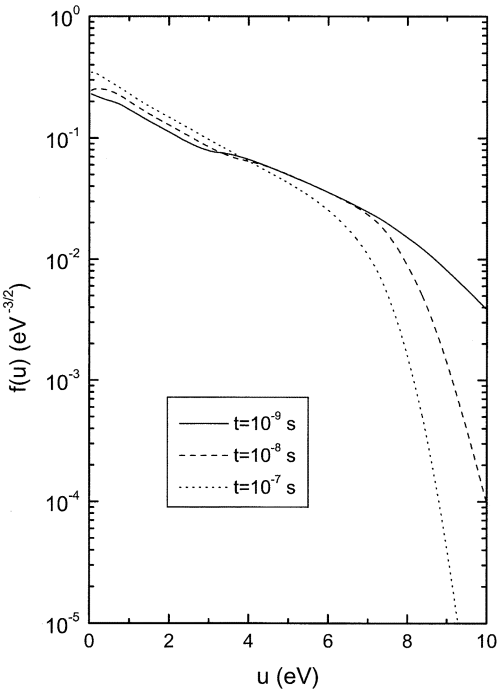

Fig. 6. The same as in Fig. 2, but for the conditions of [23]: $\omega/2\pi = 2.45$ GHz, $p = 2$ torr, $R = 0.8$ cm and $n_e(0) = 5 \times 10^{11}$ cm^{-3}. The values of E_e/N and T_V are 1.36×10^{-15} V·cm^2 and 21 100 K, respectively.

eV. This is the origin of the dip in the EEDF at 4 eV. It is worth mentioning that a local minimum in $f(u)$, very similar in shape to the one displayed in Fig. 3, was measured experimentally for a nitrogen postdischarge in [11].

One question that may arise is why does not the dip get deeper and deeper as the EEDF evolves. The answer is that $\nu(u)$ is not constant in time. In fact, in the interval 0–4 eV the electrons lose their energy mainly in inelastic collisions with the vibrational levels, but, on the other hand, they gain energy in superelastic collisions again with the vibrational levels. Therefore, an equilibrium between the EEDF and the VDF is induced in this energy range, so that after a certain time ν is vanishingly small in the range $u \leq 4$ eV. When this happens the electron temperature T_e of the distribution for $0 \leq u \leq 4$ eV merely reflects the vibrational temperature. This effect was pointed out in [15] and used in [10] to derive the vibrational temperature in the afterglow from the slope of the measured EEDF in this vibrational excitation region. The settling of the equilibrium between both distribution functions is patent in Fig. 5, were $\nu(u)$ is depicted for three different instants in the afterglow. It can be seen that the low-energy part of the EEDF reaches a quasi-stationary state for times as short as $t \sim 10^{-7}$ s.

The formation of the dip in the EEDF only takes place under certain specific conditions, related to the population of the high-energy ($u \geq 6.2$ eV) tail of the distribution function, as it can be seen in Figs. 6–8. These figures are the same as Figs. 3–5 but now for the set of parameters used in [23], corresponding to $\omega/2\pi = 2.45$ GHz, $p = 2$ torr, $R = 0.8$ cm, and $n_e(0) = 5 \times 10^{11}$ cm^{-3}. For these conditions, the calculated values from the model for E_e/N and T_V are $E_e/N = 1.36 \times 10^{-15}$ V·cm^2 and $T_V = 21100$ K. As it is shown in Fig. 6, these values are high enough to ensure a

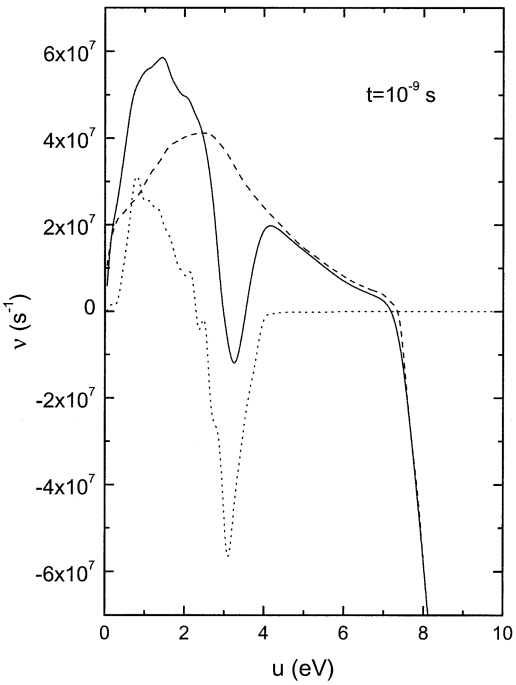

Fig. 7. The same as in Fig. 4, but for the conditions of Fig. 6.

highly populated tail of the EEDF under discharge conditions, and there is no dip formation during the relaxation process. What happens is that when one $u \geq 6.2$ eV electron loses its energy in an inelastic collision for excitation of an electronic excited state, it will appear in the distribution as an electron with $u \leq 4$ eV. In this way, if the fraction of high-energy electrons is appreciable, the arrival of low-energy electrons resulting from the excitation of the electronic states is enough

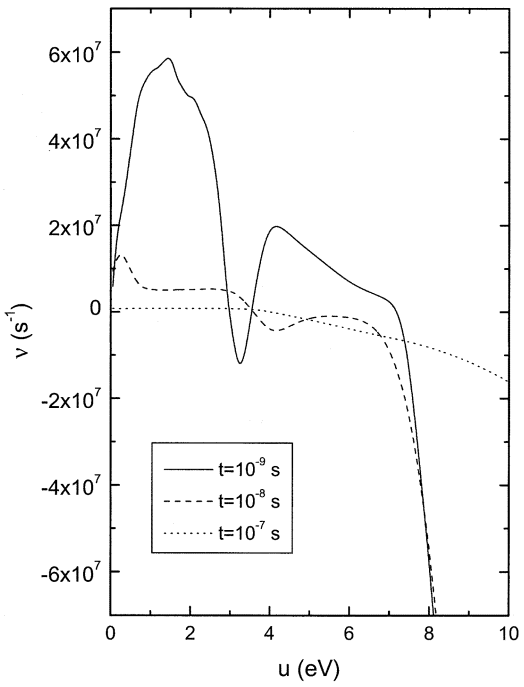

Fig. 8. The same as in Fig. 5, but for the conditions of Fig. 6.

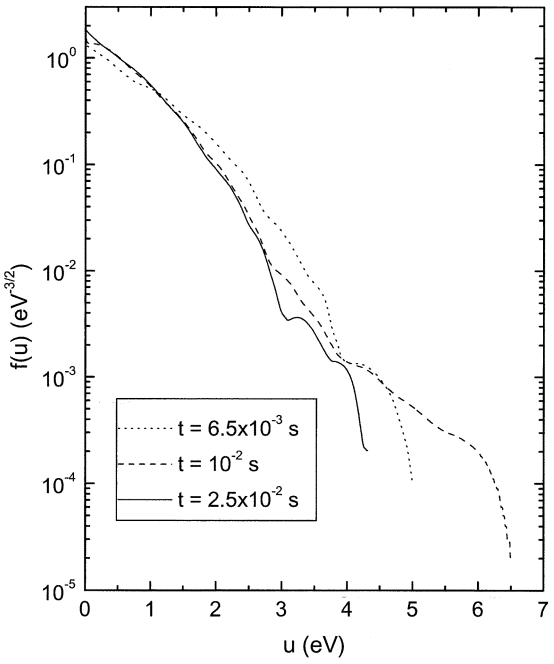

Fig. 9. Measured EEDFs in the same conditions as in Fig. 1, for the following instants in the afterglow: $t = 6.5 \times 10^{-3}$ s $(\cdots)$; 10^{-2} s $(--)$; and 2.5×10^{-2} s $(—)$.

to compensate for the loss of electrons at $u \simeq 2$–4 eV due to the e-V collisions. The effect is illustrated in Fig. 7, where the contribution of the excitation of the electronically excited states to the gain of low-energy electrons is clear. It can be immediately verified that this contribution is very small for the conditions of Fig. 4. Finally, Fig. 8 shows the evolution of $\nu(u)$ with time. This figure confirms the formation of the quasi-stationary state for the low-energy electrons at $t \sim 10^{-7}$ s, when the EEDF and the VDF reach an equilibrium.

B. Afterglow Times $t > 10^{-6}$ s

A comparison between theory and experiment is already possible for $t \gtrsim 10^{-3}$ s. Fig. 9 shows the measured EEDFs at different positions in the flowing afterglow with flow rate $Q = 1.5$ slm, $z = 12.5$ cm, 17.5 cm, and 27.5 cm, corresponding, respectively, to $t = 6.5 \times 10^{-3}$ s (dotted curve), 10^{-2} s (dashed curve) and 2.5×10^{-2} s (full curve). It should be noted that all measurements of the EEDF below 10^{-4} should be considered as merely indicative only, since the attainable EEDF resolution depends on the second derivative of the ionic current and this rapidly increases in relative value at high electron energies. This is the first experimental determination of the complete EEDF in the SLA and shows that the electron population is significant only for electrons in the energy range of $u \leq 6$ eV. From this figure the assertion of an equilibrium between the EEDF and the VDF in the low-energy region ($u \leq 4$ eV) is experimentally confirmed, since the measured EEDFs do not vary significantly from one point to the other. However, notice that our calculations predict a quasi-stationary state in the vibrational excitation region of the EEDF for times as short as $t \simeq 10^{-7}$ s, but that a global equilibrium is set only at $t \sim 10^{-6}$ s (see Fig. 2). This is in agreement with our previous calculations [23], but at the moment we do not have a direct experimental confirmation of it. Eventhough, recent measurements of the electron temperature T_e in a purely inductively coupled discharge point in this direction [45]. The measured EEDFs from Fig. 9 suggest the existence of some structure around 4 eV, similar to the one obtained theoretically for the first instants of the postdischarge. However, for the large afterglow times represented in Fig. 9, the presence of such structure cannot be ascribed exclusively to the mechanism described in the previous section (see Fig. 3 and discussion), since the equilibrium resulting from the e-V collisions has been already established for a long time. One possible explanation of this effect at large t is the gain of energy by electrons in superelastic collisions with $N_2(A\,^3\Sigma_u^+)$ metastables. These superelastic collisions provide the introduction of electrons in the EEDF with energies close to 5 eV [8] and can be in the origin of a maximum in the EEDF that can broad from 4 to 5.5 eV, as it has been experimentally observed in [8] and [15]. Of course, new measurements of the EEDF up to $u \simeq 6$ eV are desirable to verify our results, and work is now in progress to calculate the EEDF including these superelastic collisions.

Figs. 10 and 11 show the comparison between the calculated and measured EEDFs at $t = 6.5 \times 10^{-3}$ and 10^{-2} s. For values of the electron energy $u \leq 4$ eV, the slope of the EEDF essentially reflects the value of T_V, which practically remains constant from the discharge [25]. The very good agreement between the model predictions and the experimental results is hence a confirmation of the correctness of our discharge model in the calculation of the initial VDF. Nevertheless, we must note that the case represented in Fig. 11 corresponds to the upper limit of validity of the assumption of a constant vibrational temperature in the postdischarge [25]. Therefore, the value of T_V used in the calculation of the EEDF is likely to be slightly overestimated.

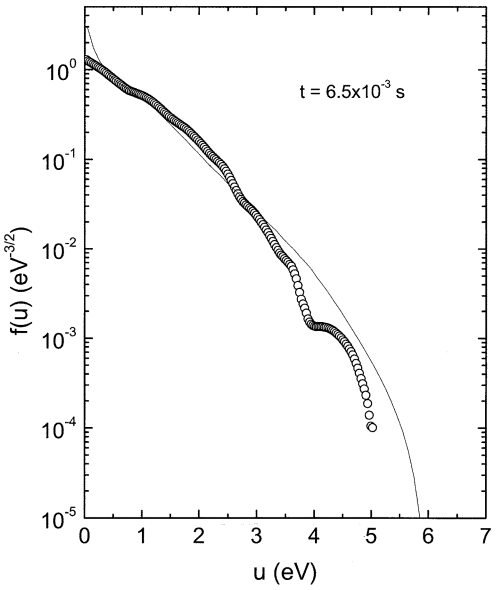

Fig. 10. Measured (∘) and calculated (—) EEDFs for the same conditions as in Fig. 1, at $t = 6.5 \times 10^{-3}$ s.

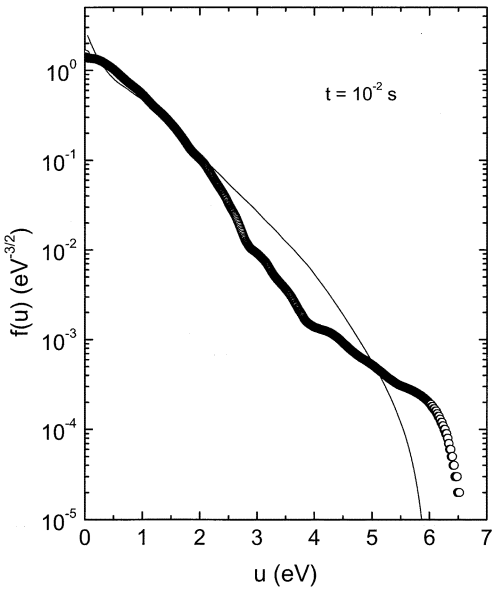

Fig. 11. Measured (∘) and calculated (—) EEDFs for the same conditions as in Fig. 1, at $t = 10^{-2}$ s.

C. Electron Density and Kinetic Temperature

Fig. 12 shows the electron density calculated from the time-dependent Boltzmann equation, by including (full curves) and neglecting (dashed curves) the creation of new electrons in reactions (1) and (2), together with the interferometry measurements from [16] (open circles) and our probe measurements (black squares). There is a very good agreement between both measurements, which confirm the applicability of the present methodology for the EEDF measurements. This agreement is extended to the theoretical calculations when the production of secondary electrons is considered in the afterglow. In particular, the no-monotonic behavior for n_e previously observed in [13] and [16] is obtained as a result of the formation of $N_2(A\ ^3\Sigma_u^+)$

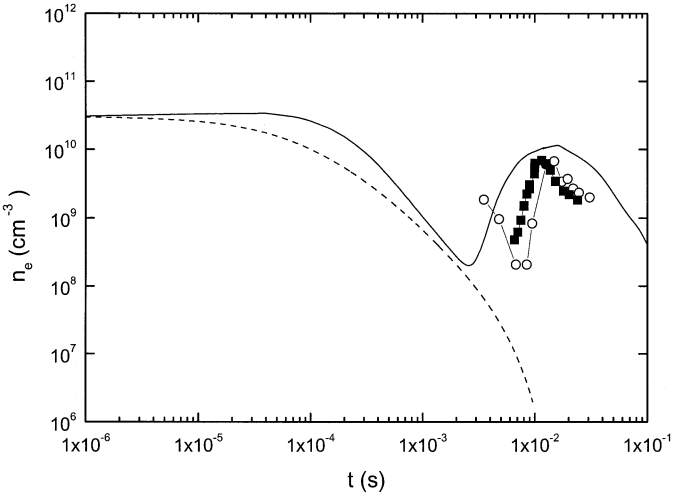

Fig. 12. Temporal evolution of the electron density as derived from our probe measurements (■), the measured data from [16] (∘) and our model predictions, when reactions (1) and (2) are included (—) and neglected (– –).

and $N_2(a'\ ^1\Sigma_u^-)$ states in reactions (10) and (11) followed by ionization through (1) and (2) [25], and in a smaller extent also by reactions (8) and (9). A detailed analysis of the effect of reactions (10) and (11) in the kinetics of the heavy-particles was presented in [25], where it was demonstrated that only reactions involving ground-sate molecules vibrationally excited in high v levels, as high as $v \gtrsim 35$, can be responsible for the observed maxima in the concentration of various species, occurring downstream from the discharge after a dark zone [16] and [17]. The dashed curve in Fig. 12 shows that slow electrons remain for a long time in the afterglow, up to $t \sim 10^{-3}$ s, even in the absence of the Penning reactions. This is a consequence of the large characteristic times for ambipolar diffusion, as calculated in [23] and measured experimentally in the breakdown time delay experiment reported in [22] and in a pulsed RF discharge in [9], so that the frequency for electron losses by diffusion is relatively small. The presence of a significant number of slow electrons for a long time makes it possible that electron stepwise excitation processes, typically with energies thresholds up to 2–3 eV, are effective under postdischarge conditions, as it was first suggested in [46] and [47] and calculated theoretically in [23]. However, these stepwise collisions cannot produce additional ionization in the postdischarge.

Fig. 13 shows the calculated electron kinetic temperature as a function of the afterglow time, with the same notation as in Fig. 12. It can be confirmed that in spite of the very fast equilibrium between low-energy electrons and the VDF, which settles for $t \sim 10^{-7}$ s, a quasi-stationary EEDF in the full range of energy only establishes itself at $t \sim 10^{-6}$ s (see also Fig. 2). At that moment $T_e \simeq T_V \simeq$ *constant*. A very similar curve for the evolution of T_e in the afterglow was recently obtained experimentally in [45] for the case of a pulsed inductive discharge. Notice as well that a high value for T_e, of the order of one electronvolt during the time interval $t \sim 10^{-6} - 10^{-4}$ s, has been previously measured in the nitrogen afterglow of an RF pulsed discharge at $p = 0.2$ torr [9]. The insert in this figure shows the comparison between the calculated values and the ones deduced

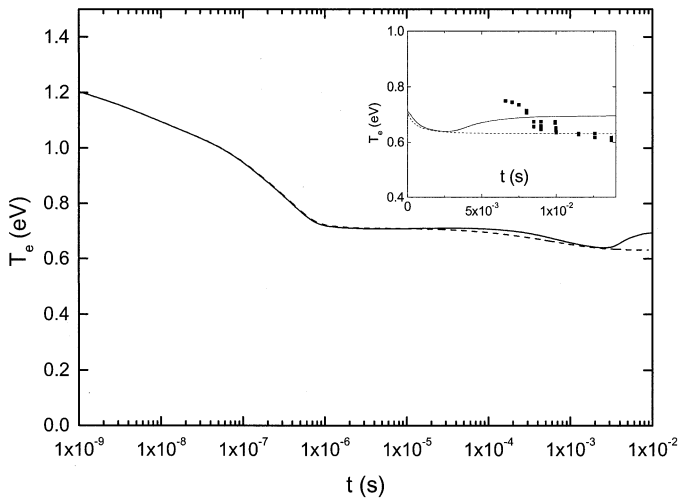

Fig. 13. Temporal evolution of the electron kinetic temperature, for the same conditions as in Fig. 1. The full and dashed curves are as in Fig. 12 and the symbols correspond to the experimental measurements.

from the present experimental probe measurements. The agreement is excellent, thus stressing the importance of both theoretical and experimental studies.

V. Conclusion

In this paper, we have developed a kinetic model to study the relaxation of the EEDF in the nitrogen afterglow. The time-dependent electron Boltzmann equation was solved taking into account the creation of new electrons in Penning reactions involving the metastable states $N_2(A\,^3\Sigma_u^+)$ and $N_2(a'\,^1\Sigma_u^-)$. The temporal evolution of the concentration of these two states was obtained from a detailed model for the relaxation of the heavy-particles in the afterglow. The investigation was complemented with the experimental determination of the EEDF and the electron density at different positions in the postdischarge.

It was shown that in some circumstances, related essentially with the population of the high-energy tail of the distribution, the EEDF exhibits a peculiar dip around $u \simeq 4$ eV for $t \sim 10^{-8} - 10^{-7}$ s. The dip occurs when the gain of electrons at $u = 2$–4 eV, resulting from the excitation of electronically excited states by high-energy electrons, is not high enough to compensate for the losses due to vibrational excitation. In this way, the formation of the dip strongly depends on the values of E_e/N and T_V.

It was further confirmed that in the early instants of the afterglow, as short as $t \sim 10^{-7}$ s, the EEDF is Maxwellian (with $T_e \simeq T_V$) for $u \leq 4$ eV, since the energy balance of the electrons is defined by the heating and cooling as a result of excitation and de-excitation processes involving vibrational levels. A full equilibrium between the EEDF and the VDF is attained at $t \sim 10^{-6}$ s, when the EEDF reaches a quasi-stationary state.

The electron density has been shown to have a no-monotonic behavior, passing through a maximum after an initial stage of slow decay. The formation of new electrons is related to the V-V pumping-up effect, since the highly excited vibrational levels $N_2(X\,^1\Sigma_g^+, v \gtrsim 35)$, not present under discharge conditions, become available in the afterglow to participate in reactions that create $N_2(A\,^3\Sigma_u^+)$ and $N_2(a'\,^1\Sigma_u^-)$ metastables. Ionization then takes place via reactions

$$N_2(A\,^3\Sigma_u^+) + N_2(a'\,^1\Sigma_u^-) \longrightarrow N_2(X\,^1\Sigma_g^+) + N_2^+ + e.$$

and

$$N_2(a'\,^1\Sigma_u^-) + N_2(a'\,^1\Sigma_u^-) \longrightarrow N_2(X\,^1\Sigma_g^+) + N_2^+ + e.$$

The permanence of slow electrons for very long times in the afterglow (at least up to $t \sim 10^{-3} - 10^{-2}$ s) suggests their involvement in low-threshold processes, such as vibrational or stepwise excitation.

As presented in this paper, the description of the electron kinetics in the nitrogen afterglow and its interplay with the heavy-particle kinetics is already rather complex, but it is, of course, far from complete. In particular, it is desirable to include the electron excitation of states $N_2(B\,^3\Pi_g)$ and $N_2(C\,^3\Pi_u)$ from $N_2(A\,^3\Sigma_u^+)$ in the set of equations describing the evolution of the heavy-particles in the postdischarge, as well as to verify the possible effect of superelastic collisions of electrons with $N_2(A\,^3\Sigma_u^+)$ molecules in the time-evolution of the EEDF. Future work should concentrate on these points, in order to obtain an improved understanding of the basic mechanisms taking place in the nitrogen afterglow.

References

[1] A. Ricard, J. E. Oseguera-Pena, L. Falk, H. Michel, and M. Gantois, "Active species in microwave postdischarge for steel-surface nitriding," *IEEE Trans. Plasma Sci.*, vol. 18, pp. 940–944, Dec. 1990.

[2] B. Mutel, J. Grimblot, O. Dessaux, and P. Goudmand, "XPS investigations of nitrogen-plasma-treated polypropylene in a reactor coupled to the spectrometer," *Surface Interface Anal.*, vol. 29, pp. 401–406, 2000.

[3] J. G. E. Beale and H. P. Broida, "Spectral study of a visible, short-duration afterglow in nitrogen," *J. Chem. Phys.*, vol. 31, pp. 1030–1034, 1959.

[4] P. Supiot, O. Dessaux, and P. Goudmand, "Spectroscopic analysis of the nitrogen short-lived afterglow induced at 433 MHz," *J. Phys. D: Appl. Phys.*, vol. 28, pp. 1826–1839, 1995.

[5] H. P. Broida, "Double probe measurements of ionization in active nitrogen," *J. Chem. Phys.*, vol. 36, pp. 236–238, 1962.

[6] H. H. Brömer and F. Döbler, "Eine modellvorstellung für das auroral afterglow und das pink afterglow," *Zeischrift für Physik*, vol. 185, pp. 278–294, 1965.

[7] S. L. Chen and J. M. Gooddings, "Electrostatic probe studies of the nitrogen pink afterglow," *J. Chem. Phys.*, vol. 50, pp. 4335–4342, 1969.

[8] N. A. Gorbunov, N. B. Kolokolov, and A. A. Kudryavtsev, "Measurement of the electron energy distribution in a nitrogen afterglow plasma," *Sov. Phys. Tech. Phys.*, vol. 33, pp. 1104–1105, 1988.

[9] G. Dilecce and S. De Benedictis, "Relaxation of the electron energy in the post-discharge of an He-N_2 misture," *Plasma Sources Sci. Technol.*, vol. 2, pp. 119–122, 1993.

[10] A. A. Kudryavtsev and A. I. Ledyankin, "On the electron and vibrational temperatures in a nitrogen afterglow plasma," *Physica Scripta*, vol. 53, pp. 597–602, 1996.

[11] T. Kimura, K. Ohe, and M. Nakamura, "Formation of dip structure of electron energy distribution function in diffused nitrogen plasmas," *J. Phys. Soc. Jpn.*, vol. 67, pp. 3443–3449, 1998.

[12] F. M. Dias and T. K. Popov, "Iterative method of evaluating the electron energy distribution function from probe measurements under collisional conditions," *Vacuum*, vol. 69, pp. 159–163, 2002.

[13] L. S. Bogdan, S. M. Levitskii, and E. V. Martysh, "Nonmonotonic variation of the electron density in the decaying plasma of a pulsed discharge in nitrogen," *Tech. Phys.*, vol. 38, pp. 532–534, 1993.

[14] S. I. Gritisin, I. A. Kossyi, V. P. Silakov, and N. M. Tarasova, "The decay of the plasma produced by a freely localized microwave discharge," *J. Phys. D: Appl. Phys.*, vol. 29, pp. 1032–1034, 1996.

[15] N. A. Dyatko, I. V. Kochetov, and A. P. Napartovich, "Electron energy distribution function in decaying nitrogen plasmas," *J. Phys. D: Appl. Phys.*, vol. 26, pp. 418–423, 1993.

[16] N. Sadeghi, C. Foissac, and P. Supiot, "Kinetics of $N_2(A\,^3\Sigma_u^+)$ molecules and ionization mechanisms in the afterglow of a flowing N_2 microwave discharge," *J. Phys. D: Appl. Phys.*, vol. 34, pp. 1779–1788, 2001.

[17] D. Blois, P. Supiot, M. Barj, A. Chapput, C. Foissac, O. Dessaux, and P. Goudmand, "The microwave source's influence on the vibrational energy carried by $N_2(X\,^1\Sigma_g^+)$ in a nitrogen afterglow," *J. Phys. D: Appl. Phys.*, vol. 31, pp. 2521–2531, 1998.

[18] C. Gorse, M. Capitelli, and A. Ricard, "On the coupling of electron and vibrational energy distributions in H_2, N_2, and CO post discharges," *J. Chem. Phys.*, vol. 82, pp. 1900–1906, 1985.

[19] C. Gorse and M. Capitelli, "Coupled electron and excited-state kinetics in a nitrogen afterglow," *J. Appl. Phys.*, vol. 62, pp. 4072–4076, 1987.

[20] S. K. Dhali and L. H. Low, "Transient analysis of bulk nitrogen glow discharge," *J. Appl. Phys.*, vol. 64, pp. 2917–2926, 1988.

[21] J. Borysow and A. V. Phelps, "Electric field strengths, ion energy distributions, and ion density decay for low-pressure, moderate-current nitrogen discharges," *Phys. Rev. E*, vol. 50, pp. 1399–1412, 1994.

[22] V. L. Marković, Z. L. Petrović, and M. M. Pejović, "Modeling of charged particle decay in nitrogen afterglow," *Plasma Sources Sci. Technol.*, vol. 6, pp. 240–246, 1997.

[23] V. Guerra, P. A. Sá, and J. Loureiro, "Relaxation of the electron energy distribution function in the afterglow of a N_2 microwave discharge including space-charge field effects," *Phys. Rev. E*, vol. 63, pp. 046 404-1–046 404-13, 2001.

[24] ——, "Electron and metastable kinetics in the nitrogen afterglow," in *Proc. XVIth Europhysics Conf. Atomic and Molecular Physics of Ionized Gases/5th Int. Conf. Reactive Plasmas Joint Meeting*, vol. 1, 2002, pp. 21–22.

[25] ——, "Electron and metastable kinetics in the nitrogen afterglow," *Plasma Sources Sci. Technol.*, 2003, to be published.

[26] V. Guerra and J. Loureiro, "Electron and heavy particle kinetics in a low pressure nitrogen glow discharge," *Plasma Sources Sci. Technol.*, vol. 6, pp. 361–372, 1997.

[27] V. Guerra, P. A. Sá, and J. Loureiro, "Role played bt the $N_2(A\,^3\Sigma_u^+)$ metastable in stanionary N_2 and N_2-O_2 discharges," *J. Phys. D: Appl. Phys.*, vol. 34, pp. 1745–1755, 2001.

[28] V. Guerra, E. Tatarova, and C. M. Ferreira, "Kinetics of metastable atoms and molecules in N_2 microwave discharges," *Vacuum*, vol. 69, pp. 171–176, 2002.

[29] L. C. Pitchford and A. V. Phelps, "Electron swarms in N_2 at high E/N," *Bull. Amer. Phys. Soc.*, vol. 27, p. 109, 1982.

[30] J. Loureiro and C. M. Ferreira, "Coupled electron energy and vibrational distribution functions in stationary N_2 discharges," *J. Phys. D: Appl. Phys.*, vol. 19, pp. 17–35, 1986.

[31] ——, "Electron excitation rates and transport parameters in direct-current N_2 discharges," *J. Phys. D: Appl. Phys.*, vol. 22, pp. 67–75, 1989.

[32] E. Tatarova, F. M. Dias, C. M. Ferreira, and A. Ricard, "On the axial structure of a nitrogen surface wave sustained discharge: Theory and experiment," *J. Appl. Phys.*, vol. 85, pp. 49–62, 1999.

[33] V. Guerra, E. Tatarova, F. M. Dias, and C. M. Ferreira, "On the self-consistent modeling of a traveling wave sustained nitrogen discharge," *J. Appl. Phys.*, vol. 91, pp. 2648–2661, 2002.

[34] L. C. Pitchford and A. V. Phelps, "Comparative calculations of electron-swarm properties in N_2 at moderate E/N values," *Phys. Rev. A*, vol. 25, pp. 540–554, 1982.

[35] P. A. Sá and J. Loureiro, "A time-dependent analysis of the nitrogen afterglow in N_2 and N_2-Ar microwave discharges," *J. Phys. D: Appl. Phys.*, vol. 30, pp. 2320–2330, 1997.

[36] J. Loureiro, P. A. Sá, and V. Guerra, "Role of long-lived $N_2(X\,^1\Sigma_g^+, v)$ molecules and $N_2(A\,^3\Sigma_u^+)$ and $N_2(a'\,^3\Sigma_u^-)$ states in the light emissions of a N_2 afterglow," *J. Phys. D: Appl. Phys.*, vol. 34, pp. 1769–1778, 2001.

[37] P. A. Sá, V. Guerra, J. Loureiro, and N. Sadeghi, "Self-consistent modeling of a flowing nitrogen microwave discharge for interpretation of afterglow data," in *Proc. XVIth Europhysics Conf. Atomic and Molecular Physics of Ionized Gases/5th Int. Conf. Reactive Plasmas Joint Meeting*, vol. 2, 2002, pp. 91–92.

[38] C. E. Treanor, J. W. Rich, and R. G. Rehm, "Vibrational relaxation of anharmonic oscillators with exchange-dominated collisions," *J. Chem. Phys.*, vol. 48, pp. 1798–1807, 1968.

[39] M. Cacciatore and M. Dilonardo, "Nonequilibrium vibrational populations of diatomic species in electrical discharges: Effects on the dissociation rates," *Chem. Phys.*, vol. 24, pp. 417–427, 1977.

[40] F. M. Dias, "Use of emissive probes in HF plasmas," in *Microwave Discharges: Fundamentals and Applications*. ser. NATO ASI, C. M. Ferreira and M. Moisan, Eds. New York: Plenum, 1993, vol. B-302, pp. 291–302.

[41] F. M. Dias, E. Tatarova, and C. M. Ferreira, "Spatially resolved experimental investigation of a surface wave sustained discharge in nitrogen," *J. Appl. Phys.*, vol. 83, pp. 4602–1235, 1998.

[42] T. Popov, D. Ivanova, and M. Tchernookov, "On negative ions langmuir probe measurements in an Ar+4%CF_4 currentless plasma," in *Advanced Techniques Based on Wave and Bean Generated Plasmas*. ser. NATO Science, H. Schlüter and A. Shivarova, Eds. Norwell, MA: Kluwer, 1999, vol. 3/67, pp. 473–474.

[43] N. A. Gorbunov, N. B. Kolokolov, and A. A. Kudryavtsev, "Probe measurements of the electron energy distribution function at intermediate and high pressures," *Sov. J. Plasma Phys.*, vol. 15, pp. 881–885, 1989.

[44] C. M. Ferreira and M. Moisan, "The similarity laws for the maintenance field and the absorbed power per electron in low-pressure surface wave produced plasmas and their extension to HF plasmas in general," *Physica Scripta*, vol. 38, pp. 382–399, 1988.

[45] G. Dilecce, P. A. Ambrico, R. Bektursunova, and S. De Benedictis, "Decay of electron temperature in a pulsed purely inductive discharge," in *Proc. XVIth Europhysics Conf. Atomic and Molecular Physics of Ionized Gases/5th Int. Conf. Reactive Plasmas Joint Meeting*, vol. 1, 2002, pp. 211–212.

[46] S. De Benedictis and G. Dilecce, "Vibrational relaxation of $N_2(C, v)$ state in N_2 pulsed rf discharge: Electron impact and pooling reactions," *Chem. Phys.*, vol. 192, pp. 149–162, 1995.

[47] G. Cartry, L. Magne, and G. Cernogora, "Experimental study and modeling of a low-pressure N_2-O_2 time afterglow," *J. Phys. D: Appl. Phys.*, vol. 32, pp. 1894–1907, 1999.

Vasco Guerra was born in Torres Vedras, Portugal, on December 12, 1968. He received the degree in physical engineering and the Ph.D. degree in physics from the Instituto Superior Técnico (IST), Lisbon Technical University, Lisbon, in 1991 and 1998, respectively.

Since 1998, he has been Assistant Professor with the Physics Department at IST. His research interests are focused on the modeling of kinetic processes in molecular plasmas, including electron and heavy-particle kinetics and gas-surface processes.

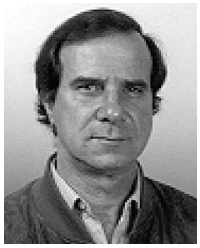

Francisco M. Dias was born in Portimão, Portugal, on March 28, 1949. He received the degree in electrical engineering from Instituto Superior Técnico (IST), Lisbon Technical University, Lisbon, in 1971. He received the research degree equivalent of the Ph.D. degree in physics from INIC, 1988.

Since 1972, he has been a Researcher at IST and became "Investigador Principal" in 1997. From 1974 until 2002, he lectured on propagation and radiation of electromagnetic waves at the Military Academy, where he became Associated Professor in 1991. He has been working in hollow cathode arcs and surface wave discharges, and his main research interests concern plasma diagnostics.

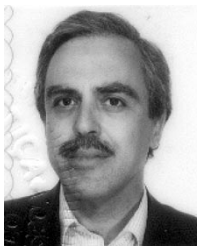

Jorge Loureiro was born in Lisbon, Portugal, in 1951. He received the degree in electrical engineering and the Ph.D. degree in physics from the Instituto Superior Técnico (IST), Lisbon Technical University, Lisbon, in 1976 and 1987, respectively.

Since 1993, he has been Associate Professor with the Physics Department at IST. His work is concentrated in the kinetic modeling of dc and HF discharges, in atomic and molecular gases, and their mixtures, such as N_2-H_2, N_2-O_2, N_2-Ar, N_2-CH_4, SF_6-N_2, etc.

Paulo Araújo Sá was born in Porto, Portugal, on June 29, 1960. He received the degree in applied physics from Sciences Faculty of Porto University, Porto, Portugal, in 1984, and the Ph.D. degree in physics from Instituto Superior Técnico, Lisbon Technical University, Lisbon, Portugal, in 1994.

Since 1984 he has been in the Faculty of Engineering of Porto University where he is now Assistant Professor with the Physics Department. His present research interests concern the kinetic modeling of microwave gas discharges and postdischarges.

Philippe Supiot was born in Angers, France, on September 7, 1963. He received the degree in physics and cold plasma physical-chemistry from Paris-Sud University, Paris, France, and the Doctor of Science degree from Lille University, Lille, France, in 1993.

Since 1994, he has been a Senior Researcher and Chief of Scientific Group (since 2000) with the Chemistry Departement at Lille I University. His scientific interest is the experimental investigation for understanding of kinetic processes in discharges and afterglows in molecular gases and plasma applications in the field of surface treatment and thin film deposition.

Chrsitian Dupret graduated in physics from the "Conservatoire des Arts et Métiers," Paris, France, in 1970. He received the "Diplome Supérieur de Recherche" in physics from the University of Lille I, Lille, France, in 1993.

He is currently an Electronics Engineer in the GePIFReM laboratory, Lille. His research activities are in the field of study and application of RF and microwave coupling devices for plasma sources production.

Tsviatko K. Popov was born in Kazanlak, Bulgaria, on April 11, 1953. He received the degree in physics and the Ph.D. from the St. Kliment Ohridski University of Sofia, Sophia, Bulgaria, in and 1983, respectively.

Since 1986, he is Associate Professor (Reader) with the Faculty of Physics, Sofia University. His scientific interests are optical and Langmuir-probe diagnostics of low-temperature plasma and gas discharges and especially determination of the electron energy distribution function (EEDF) and cross sections or rate coefficients for inelastic collisions in low-temperature plasma from experimental data.